European Journal of Cell Biology 98 (2019) 103–115

Contents lists available at ScienceDirect

European Journal of Cell Biology

journal homepage: www.elsevier.com/locate/ejcb

Research paper

# Stage-specific testes proteomics of *Drosophila melanogaster* identifies essential proteins for male fertility

Stefanie M.K. Gärtner[a,1], Tim Hundertmark[a,1], Hendrik Nolte[b], Ina Theofel[a,c], Zeynep Eren-Ghiani[a], Carolin Tetzner[a], Timothy B. Duchow[a], Christina Rathke[a], Marcus Krüger[b,2], Renate Renkawitz-Pohl[a,2,*]

[a] Philipps-Universität Marburg, Fachbereich Biologie, Entwicklungsbiologie, Karl-von-Frisch Str. 8, 35043, Marburg, Germany
[b] Institute for Genetics and Cologne Excellence Cluster on Cellular Stress Responses in Aging-Associated Diseases (CECAD), University of Cologne, Joseph-Stelzmann-Strasse 26, 50931 Cologne, Germany, Center for Molecular Medicine (CMMC), University of Cologne, 50931, Cologne, Germany
[c] MRC London Institute of Medical Sciences (LMS), Du Cane Road, London W120NN, UK, Institute of Clinical Sciences (ICS), Faculty of Medicine, Imperial College London, Du Cane Road, London, W12 0NN, UK

ARTICLE INFO

*Keywords:*
transition-like protein
Proteasome Assembly Chaperone 1
microtubule-binding protein
nuclear shaping
THEG
Y chromosome

ABSTRACT

Spermiogenesis in *Drosophila melanogaster* is a highly conserved process and essential for male fertility. In this haploid phase of spermatogenesis, motile sperm are assembled from round cells, and flagella and needle-shaped nuclei with highly compacted genomes are formed. As transcription takes place mainly in spermatocytes and transcripts relevant for post-meiotic sperm development are translationally repressed for days, we comparatively analysed the proteome of larval testes (only germ cell stages before meiotic divisions), testes of 1–2-day-old pupae (germ cell stages before meiotic divisions, meiotic and early spermatid stages) and adult flies (germ cell stages before meiotic divisions, meiotic and early spermatid stages, late spermatids and sperm). We identified 6,171 proteins; 61 proteins were detected solely in one stage and are thus enriched, namely 34 in larval testes, 77 in pupal testes and 214 in adult testes. To substantiate our mass spectrometric data, we analysed the stage-specific synthesis and importance for male fertility of a number of uncharacterized proteins. For example, Mst84B (gene *CG1988*), a very basic cysteine- and lysine-rich nuclear protein and was present in the transition phase from a histone-based to a protamine-based chromatin structure. *CG6332* encodes d-Theg, which is related to the mouse tHEG and human THEG proteins. Mutants of *d-Theg* were sterile due to the lack of sperm in the seminal vesicles. Our catalogue of proteins of the different stages of testis development in *D. melanogaster* will pave the road for future analyses of spermatogenesis.

## 1. Introduction

In spermatogenesis, functional motile spermatozoa develop from an initially undifferentiated germ cell. The characteristic features of this process are highly conserved in *Drosophila melanogaster* and mammals (Rathke et al., 2014). Stem cells divide to form new stem cells and spermatogonia, i.e. differentiating germ cells. These spermatogonia proceed first through a mitotic amplification phase and then enter the extended meiotic prophase as spermatocytes (Fuller, 1993). After meiotic divisions, spermatids differentiate within days (*D. melanogaster*) or weeks (mammals) to form motile sperm with highly condensed chromatin (Rathke et al., 2014).

It is obvious that during germ cell differentiation, a plethora of proteins have to be newly synthesized in a stage-specific manner. However, data on protein expression in the testis is scarce due to technological and methodical limitations. Until recently, proteomic research on whole testis tissue of different species entailed 2-D gels and subsequent mass spectrometry of excised protein spots. With this technique, 232 proteins were identified in testes of *D. melanogaster*, 1,108 were identified in *Drosophila* sperm (in this case, by solubilizing purified whole sperm in the presence of trypsin and directly introducing the sample into the mass spectrometer, Dorus et al.; 2006; Wasbrough et al. 2010; for a review, see Karr 2007), 447 were observed in pig testes (Huang et al., 2005), 504 were identified in mouse testes (Zhu et al.,

* Corresponding author.
*E-mail address:* renkawit@biologie.uni-marburg.de (R. Renkawitz-Pohl).
[1] shared first authorship.
[2] joint last authors.

https://doi.org/10.1016/j.ejcb.2019.01.001
Received 6 September 2018; Received in revised form 10 January 2019; Accepted 10 January 2019

**Table 1**
Predicted basic proteins expressed at a high level in *Drosophila* testes.

| Gene | pI (predicted) | Molecular mass (kDa; predicted) | Domain/motif (predicted) | Transcript level in adult testes (Fly Atlas) |
|---|---|---|---|---|
| *CG12860* | 9.76 | 36.6 | Cysteine rich | Very high |
| *CG4691* | 10.38 | 30.8 | Cysteine rich | Very high |
| *CG1988* | 10.48 | 60.2 | Cysteine and lysine rich | Very high |
| *CG17377* | 8.45 | 18.6 | - | Very high |
| *CG31542* | 8.63 | 21.2 | - | Very high |
| *CG31907* | 9.82 | 49.0 | Calponin homology domain, microtubule-associated protein Rp/EB, CH domain superfamily | Very high |
| *CG6332* | 10.60 | 40.5 | Testicular haploid expressed repeat | Very high |
| *CG5089* | 10.48 | 51.7 | - | Very high |
| *CG8701* | 9.66 | 27.6 | Cysteine rich | Very high |

2006), 725 were found in human testes (Li et al., 2011), and 6,198 were identified in human sperm (in 30 studies, summarized in Amaral et al., 2014). Together, these proteomes provides a comprehensive reference map for differentiated testis under normal conditions. However, the number of proteins of *Drosophila* identified to date does not come close to reflecting the number of genes that are transcribed during spermatogenesis. For example, over 2,000 genes are transcribed in spermatocytes, many for the first time in the life cycle (Lu and Fuller, 2015; Theofel et al., 2014, 2017; White-Cooper and Davidson, 2011), and in a random mutagenesis study (Wakimoto et al., 2004), mutation of at least 2,000 genes leads to male infertility. Furthermore, the proteomic datasets of whole testis tissue provide only limited information about the expression profiles of proteins at different developmental stages of germ cells, which is needed to further broaden the understanding of the process of spermatogenesis and to pinpoint the protein function to specific cell types.

Several approaches have been used to generate mRNA expression profiles specific to certain stages of spermatogenesis. Studies in mice made use of the observation that at a given day after birth, certain germ cell types are enriched in the testis (Schultz et al., 2003; Xiao et al., 2008). An earlier transcriptomics study in fruit flies took advantage of the almost chronological arrangement of the germ cells in the adult testis, which could be divided into three regions enriched with mitotic, meiotic or post-meiotic cells (Vibranovski et al., 2009). Furthermore, isolated and enriched testicular cell populations were used to generate genetic databases of rats and mice (http://mrg.genetics.washington.edu/). These methods greatly facilitated the assignment of transcripts to mitotic, meiotic, and post-meiotic stages of spermatogenesis and helped to identify yet uncharacterized transcripts that likely encode factors involved in spermatogenesis and fertility. Nevertheless, the proteins — usually the final products of gene expression — are considered to be more relevant markers for gene function. This becomes even more obvious because mRNA levels do not necessarily predict protein expression, in particular during male germ cell development.

Spermatogenesis is one of the finest examples illustrating the importance of post-transcriptional regulation of gene expression. A common feature of mammalian and fly germ cell development is an almost complete shut-down of transcription in post-meiotic stages. This block of transcription occurs at the round spermatid stage in mammals, and even earlier in flies, namely at the end of the primary spermatocyte stage (for a review, see Rathke et al., 2014). Consequently, transcripts whose products are needed in later stages of spermatogenesis have to be translationally repressed (for a review, see Renkawitz-Pohl et al., 2005; Rathke et al., 2014), and this leads to a clear discrepancy between the transcriptome and the proteome of a certain stage. Many mRNAs are translationally repressed for days until the late steps of sperm maturation. Typical examples in *Drosophila* are proteins of sperm chromatin, which are deposited between 50 and 60 h after meiotic divisions (Jayaramaiah and Renkawitz-Pohl (2005); Awe and Renkawitz-Pohl, 2010; Barckmann et al., 2013, Eren-Ghiani et al., 2015). Thus, transcriptomic research has to be complemented by proteomic approaches to evaluate the function of genes in spermatogenesis. To date, two studies in pigs and mice have aimed at identifying differentially synthesized proteins in the developing testes (Huang et al., 2011; Paz et al., 2006).

Today, proteomic approaches allow the rapid identification of proteins in complex mixtures. Peptides are separated via liquid chromatography (LC), followed by tandem mass spectrometry (MS/MS). With this approach, the human and mouse testis proteome was expanded to over 5,000 proteins (Liu et al., 2013; Huttlin et al., 2010). However, this approach has not yet been applied to the *Drosophila* model organism of spermatogenesis. In this case, it needs to be considered that the fly testis contains fewer somatic cell types than the mammalian testes.

In this study, we used single-shot proteomics to extend the number of identified proteins in the *Drosophila* testis proteome and to investigate differential protein expression in the developing testis by analysing larval, pupal and adult testis proteomes.

## 2. Material and methods

### 2.1. Fly stocks and maintenance

We used an H2 AvD-RFP; ProtamineB-eGFP double-transgenic *Drosophila melanogaster* strain (Awe and Renkawitz-Pohl, 2010). Fly strains CG2046$^{f01807}$ (BL 18477), Df(3R)Exel6145, Df(3R)Exel7283 and Df(3R)Exel7284 were obtained from the Bloomington *Drosophila* Stock Center.

The fly strains were maintained at 25 °C on standard medium. Prior to isolation of the testes for proteome analysis, the flies were cultured for one generation on standard medium containing 0.003% tetracycline to avoid *Wolbachia* sp. infection (Hoffmann and Turelli (1988)). Flies were controlled by PCR for infection with *Wolbachia* sp. using *wsp*-forward TGGTCCAATAAGTGATGAAGAAAC and *wsp*-reverse AAAAAT TAAACGCTACTCCA primers (Zheng et al., 2011). Primers for *Tpl94D* positive control were Tpl-RT-sen GAGTGCATCACGTGAATGGG and Tpl-RT-as GCCACGCTGATCCGCATTC.

### 2.2. Isolation of testes for proteome analysis

We prepared three independent biological replicates of larval, pupal and adult testes. For each proteome, we isolated 2,000 testes for each of the three biological replicates. We prepared testes manually within one week for each biological replicate. Testes were isolated from late wandering 3rd instar larvae to reduce contamination with fat body cells, from pupae at approximately 24 h after puparium formation (APF), from pupae at approximately 48 h APF and from newly eclosed flies. Isolated testes were placed in PBS containing protease inhibitor cocktail (Roche) and stored on ice for the duration of the dissection. Testes isolated from larvae, 24 h pupae and 48 h pupae were checked

for the absence or presence of ProtamineB-eGFP, which is characteristic from 48 h APF onward, with a Zeiss Axio Observer Z1 inverted microscope. The testes were carefully transferred to microcentrifuge tubes and washed three times with PBS. The PBS supernatants were discarded, and the testes samples were snap-frozen in liquid nitrogen and stored at −80 °C until processing for one-dimensional SDS-PAGE (see below). Three replicates of each testes stage were independently prepared.

### 2.3. Preparation of protein extracts for mass spectrometry

The frozen testes pellets were thawed and solubilized in sample buffer containing 4% SDS, 0.1 M Tris-HCl (pH 7.6). After shaking for 5 min at 95 °C, the samples were sonicated. The sonicated samples were incubated with shaking for 5 min at 95 °C and then centrifuged for 10 min at 10,000 × *g* in a microcentrifuge at room temperature. The supernatant was transferred to a new microcentrifuge tube. Protein concentration was estimated using the DC protein assay (Bio-Rad).

### 2.4. One-dimensional SDS-PAGE

We analysed three biological replicates of each testes stage (independent testes preparation, protein extraction and proteomics). After determination of the protein concentration, we set aside 40 µg of each testes sample for mass spectrometry. For one-dimensional SDS-PAGE, proteins were separated on a Novex NuPAGE 4–12% acrylamide gradient gel (Invitrogen). Following electrophoresis, gels were fixed in 40% methanol/10% acetic acid for 10 min and stained with the Colloidal Blue staining kit by Invitrogen according to the manufacturer's manual. The gel lanes were cut vertically and horizontally into ten fractions. For subsequent mass spectrometry analysis, proteins in the gel slices were proteolytically digested with trypsin. The resulting tryptic peptides were extracted with acetonitrile, desalted and purified using stop-and-go extraction (STAGE) tips (Rappsilber et al., 2003).

### 2.5. Protein identification by LC-mass spectrometry

Peptides were separated on an Easy nano-flow HPLC system (Thermo Fisher Scientific) with a binary buffer (buffer A: 0.1% formic acid or 0.5% acetic acid; buffer B: 80% acetonitrile, 0.1% formic acid or 0.5% acetic acid). This system was coupled to an Orbitrap- based mass spectrometer via a nano-electrospray ionization source (Velos or QExactive). Peptides were eluted from self-packed 20 cm (3 µm beads, 75 µm ID, Dr. Maisch Germany) or 50 cm (1.8 µm beads, 75 µm ID, Dr. Maisch Germany) column by linearly increasing the relative amount of buffer B from 7% to 38% within 40 min and further increasing to 65% buffer B within 10 min, followed by 5 min at 95% buffer B and then re-equilibration for 5 min to 5% buffer B. The column temperature was kept constant at 50 °C using a self-built column oven.

MS spectra in a mass range of 350–1650 *m/z* were acquired using an AGC target of 3E6 at a resolution of 70,000 at 200 *m/z*. The instrument worked in data-dependent mode; the ten most intense peaks for fragmentation (HCD or CID) in a 100–1650 *m/z* mass range were isolated. The AGC target was set to 5E5, combined with a resolution of 35,000 at 200 *m/z*, and the maximum injection time was set to 60 ms.

### 2.6. Proteome dataset composition and analysis

The complete set of raw files was processed using MaxQuant (1.5.3.8) and the implemented Andromeda search engine (Cox and Mann, 2008; Cox et al., 2011). For protein assignment, ESI-MS/MS fragmentation spectra were correlated to the UniProt fruit fly database (*Drosophila melanogaster*, complete proteome, June 2017) as well as to a list of contaminants. A maximum of two missed cleavages and a mass tolerance of 4.5 ppm and 7 ppm were set for the first and main MS/MS search, respectively. Carbamidomethyl at cysteine residues was defined as a fixed modification, and oxidation at methionine and acetylation at the N-terminus of proteins were set as variable modifications. A minimum peptide length of seven amino acids was required for identification. For quantification, a minimum ratio count of 2 was selected. The False discovery rate (FDR) was controlled to 0.01 using a target-decoy approach at the peptide-spectrum-match and protein levels and the implemented reverse algorithm. MaxQuant output text files were filtered for contaminants and reverse entries. Gene ontology based on Uniprot identifiers was annotated in Perseus software (Tyanova et al., 2016a, Tyanova et al. (2016b) Data were visualized and analysed using the in-house-developed software Instant Clue (www.instantclue.uni-koeln.de, Nolte et al., 2018).

### 2.7. Protein extraction

Protein was extracted from adult *Drosophila* testes as described in Leser et al. (2012).

For western blots, proteins were separated on 10% SDS-polyacrylamide gels following standard methods. Anti-CG2046 (dPSMG1) antibody from rabbit was used at a dilution of 1:1,000, and anti-Actin (Biomeda) was used at a dilution of 1:1,000 in 5% dry milk in Tris-buffered saline with Tween (TBST). POD-conjugated anti-rabbit antibody was subsequently applied at a dilution of 1:5,000 (Jackson Immunology). The Novex ECL chemiluminescent substrate reagent kit (Invitrogen) was used to detect the signals according to the manufacturer's recommendation.

### 2.8. Establishment of transgenic flies

We established fly constructs carrying *CG31907-eGFP*, *CG5089-eGFP*, *CG8701-eGFP* and *CG6332-eGFP*. To do this, we PCR amplified the corresponding genomic regions from 1045, 1066, 982 and 1145 bp upstream of the translation initiation codon, respectively, until the last codon; the sequence encoding eGFP was fused in-frame at the end of each open reading frame. *CG31907* and *CG6332* were cloned into pChapΔSalΔLacZ-eGFP, and transgenic flies were established by injecting constructs into $w^{1118}$ embryos. *CG5089* and *CG8701* were cloned into pUAST-attB-rfa-eGFP using the Gateway system, and transgenic flies were established by injecting constructs into *Drosophila* stock 24749 (Bloomington *Drosophila* Stock Center).

### 2.9. Fertility tests

Batches of 20 flies were tested for fertility. Each adult male (0–1 day old) was placed with three wild-type virgin females in a separate vial at 25 °C. After 6 days, the parental generation was removed. After 2 weeks, the number of vials with and without progeny was counted.

### 2.10. RT-PCR and in situ hybridization

RNA was isolated from 60 testes of adult males using TRIzol (Invitrogen). Primers for *CG6332* (*dtheg*) transcripts were as follows: 5′-primers for amplifying a 274 bp fragment by RT-PCR were CG6332-5 Fw (GGGGAGTCCATACTGAACAGAT) and CG6332-Rv (CCCACTTG GGTTTGATCTCCT); 3′-primers for amplifying a 240 bp fragment by RT-PCR were CG6332-Fw (GTGCGCGATAATGTCCACAT) and CG6332-3Rv (GATATGCGTGTTCTCGAACTC). As a control, a 372-bp fragment of β3 tubulin transcripts was amplified (fw primer: ATCATTTCCGAGGAGC ACGGC, rev primer: GCCCAGCGAGTGCGTCAATTG).

We verified the insertion of a PiggyBac element in CG2046 by PCR on genomic DNA isolated from homozygous *CG2046f01807* flies with the primer pairs 2046 F L fw (CACCATGAGCTGTCCAGGATTTGG) and pB5seq rev (CGCGCTAATTAGAAAGAGAGAG). The resulting PCR fragment was sequenced to confirm that PiggyBac was inserted between base pair 85 and base pair 86 of the open reading frame. DIG-labelled antisense RNA probes were generated using the *CG2046* open reading

frame (without introns) cloned into pCR®II-TOPO® Vector (Invitrogen) as template. Whole-mount adult testes were hybridized *in situ* according to Morris et al. (2009).

### 2.11. Antibody generation and immunofluorescence

Antibodies were raised in rabbits against peptides of CG2046 (dPSMG1) CKPKVEFKSEDIQLYRDH), CG6332 (dTheg: CLAKPKKAPK-VPKPDRGAGE) and *CG1988* (Mst84B: CDTLSHRLDQPLRSAFLEDLEK-RLNQR) (Pineda Antibody Service; http://www.pineda-abservice.de). The affinity-purified antibodies were applied in immunofluorescence stainings at the following dilutions: 1:1,000, anti-CG2046 (dPSMG1) and antiCG6332 (dTheg); and 1:10,000 anti-CG1988 (Mst84B). Squash preparations of testes, anti-histone, anti-ProtB (Doyen et al., 2013) and secondary antibodies were used as described in Gärtner et al. (2015). F-actin was visualized by rhodamine-phalloidin, and DNA was visualized with Hoechst 33258 dye. Immunofluorescence was monitored using a Zeiss AxioPlan2 microscope equipped with appropriate fluorescence filters. Recorded images were processed with Adobe PhotoshopCS2.

### 2.12. Data availability

The mass spectrometry proteomics data have been deposited in the ProteomeXchange Consortium via the PRIDE partner repository with the dataset identifier PXD010627 (Vizcaino et al., 2016).

## 3. Results and Discussion

In *Drosophila*, spermatogenesis starts from a primordial primary spermatogonium in early larval stages. This process continues uninterrupted throughout the life of the fly. The primary spermatogonia, located at the anterior end of the testis tube, undergo four cycles of mitotic divisions with incomplete cytokinesis to produce 16 primary spermatocytes enclosed by two cyst cells. The unit of the germ cells and cyst cells is called a cyst. After the meiotic divisions, each cyst contains 64 haploid spermatids that undergo dramatic morphological changes during spermiogenesis, which leads to the formation of mature sperm (Fuller et al., 1993). The appearance of new cell types at specific times during development has to be accompanied by changes in the expression of proteins.

We comparatively studied the proteomes of larval, pupal and adult testis, taking advantage of the known composition of cell types in the different stages (Gärtner et al., 2014). Larval testes contain mainly mitotic cells and cells in meiotic prophase (spermatogonia and spermatocytes). With progression of spermatogenesis, the testes gradually become enriched with later germ-cell stages. Pupal testes at 24 h APF are enriched in meiotic stages and early spermatid stages; the first protamine-positive nuclei are visible in pupal testes at 36 h APF; at 48 h APF several germ-line cysts with protamine-positive nuclei become visible (Gärtner et al., 2014). Adult testes are enriched in post-meiotic stages (late spermatids and spermatids ready for individualization with their long flagella). Besides germ cells and cyst cells, *Drosophila* testes also contain a thin sheath of pigment cells throughout their development. In larval testes, pigment cells enclose a single lumen almost entirely filled with the developing germ cells. Nascent myotubes start to cover the testes from 36 h APF onwards, while the testes of adult flies contain a tight sheath of mature muscles between the pigment cells and the germ cells (Susic-Jung et al., 2012; Rothenbusch-Fender et al., 2017). The formation of the muscle sheath is accompanied by differentiation and growth of the testis from an ovoid-shaped organ in larvae to the coiled tubular shape of the testes in adult flies (Fig. 1).

*Comprehensive proteome analysis of larval, pupal and adult testes of Drosophila by LC-MS/MS.*

We used wild-type *Drosophila* grown on medium containing tetracycline to inhibit growth of *Wolbachia* sp., a bacterium that infects germ cells and might inhibit spermatogenesis (Zheng et al., 2011). The lack of *Wolbachia* sp. DNA or transcripts was controlled by RT-PCR (Supplementary Fig. 1). To unravel the stage-specific testes proteome signature, we isolated larval testes (L3), pupal testes at 24 and 48 h APF, and adult testes (Fig. 1). Proteins were separated by SDS-PAGE and digested in the gel, followed by LC-MS/MS using an Orbitrap mass spectrometer (Fig. 1).

We identified more than 6,000 protein more than 5,000 of which were quantified in three replicates; this number of proteins greatly expands the number of fruit fly testis proteins (232 proteins) identified earlier (Takemori and Yamamoto, 2009). Quantification and identification data as well as Flybase IDs and CG numbers are reported in the Appendix. Technical reproducibility was assessed by determining the Pearson correlation coefficient between all replicates (Supplementary Fig. 2). We found an almost linear correlation between biological replicates ($r > 0.87$); we visualized this correlation matrix using hierarchical clustering. The clustering clearly separated biological replicates of larval, pupal and adult testes from each other, which indicated unique stage-specific proteomes. Protein signatures of 24 h and 48 h APF pupal samples were separated by small distances, which indicated that the technical variance of independent sample preparation was higher than the biological variance between the 24 h und 48 h APF samples. We therefore combined the results of the 24 h and 48 h APF pupal proteomes for each of the three independent biological replicates used in the following analyses (Supplementary Fig. S2). Furthermore, principal component analysis revealed a clear separation of larval, pupal and adult proteomes, which indicated that the developmental stages had unique proteomic expression profiles (Fig. 2A, Supplementary Fig. 3 shows the hierarchical clustering).

We quantified 5,359 proteins in larval testes, 5,798 proteins in pupal testes, and 5,738 proteins in adult testes, which indicated robust sample preparation and instrument performance. In addition to the class of proteins that were exclusively identified in larval (61), pupal (77) and adult (214) testes, 4,905 proteins were present in all three developmental stages (Fig. 2B; Supplementary Table 1). Moreover, 295 proteins were found — and thus enriched in the corresponding stages — in both larval and pupal testes but not in adult testes, 537 proteins were found in both pupal and adult testes but not in larval testes, and 82 proteins were found in both larval and adult testes but not in pupal testes (Fig. 2B).

We found that our larval testes samples contained abundant proteins known to be characteristic of Malpighian tubules or the larval fat body. We reasoned that such proteins would not be enriched in the pupal testes which are more easily dissected and separated from surrounding organs. Toward eliminating contaminants from proteins expressed in spermatogenic cysts, we first compared larval and pupal testes proteins and their corresponding transcripts as identified by modENCODE. Besides eliminating contaminants, we enriched for proteins relevant for stages before meiotic division by comparing the larval and pupal testes proteomes (Supplementary Table 2). We identified 294 such proteins present in both the larval and pupal testes proteomes and compared them to their transcripts identified by RNA-seq data (modENCODE, Flybase). Transcripts of these proteins were mostly present in low to moderate amounts in the adult testes. We considered that many of these proteins are relevant for stages before meiotic divisions, as larval testes contain stages from stem cells until shortly before meiotic division. Indeed, the identified proteins that were common to larval and pupal testes included, e.g. Vers [Versatile; FBgn0011335, relevant for male germ-line stem cell fate (Liu et al., 2016)] and Chinmo [FBgn0086758, sexual identity of male germ-line cyst cells (Ma et al., 2016; Grmai et al., 2018)]. We also identified numerous components of the transcriptional machinery, such as members of the Mediator complex (MED9, 11, 28, 24, 25). This is in agreement with the knowledge that MED22 is expressed in spermatocytes and is essential for male fertility; Lu and Fuller, 2016); and the transcriptional regulators tBRD-3 (FBgn0050417, Theofel et al., 2014), tPlus3 (FGgn0051703, Hundertmark et al., unpublished results and Wuc (FBgn0033770 Wake-

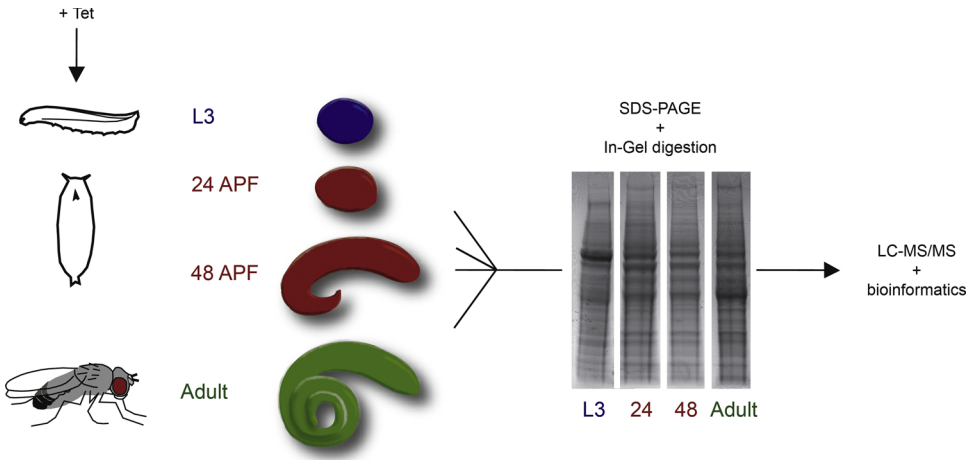


**Fig. 1.** Experimental design for the identification of proteins in *Drosophila* larval, pupal and adult testes by LC-MS/MS. Larval, pupal and adult testes of tetracycline-treated flies were isolated. Blue, third instar larval testis (L3); red, pupal testes at 24 h and 48 h APF; green, adult testis. Corresponding protein extracts were separated on SDS-polyacrylamide gels and processed for mass spectrometric analysis.

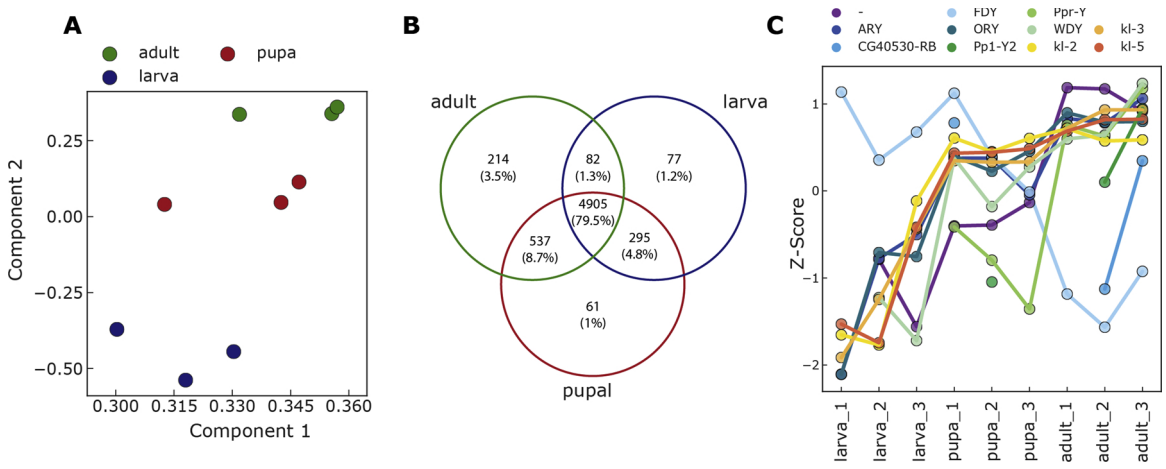


**Fig. 2.** Proteome analysis of *Drosophila* testes at selected stages of development. (A) PCA score plot showing clear segregation between biological developmental states. B) Venn diagram showing the overlap of quantified proteins between biological conditions. C) Point plot of proteins/genes encoded on the Y-chromosome. The log2 LFQ intensities were Z-score transformed. Gene names are colour coded.

up-call, Doggett et al., 2011). We identified numerous proteins with DNA- and RNA-binding potential (Supplementary Table 2). We identified known or predicted gamma tubulins, centromere-relevant proteins, e.g. mei-S332, also known as Shugoshin (FBgn0002715, Nogueira et al., 2014), sperm relevant proteins (Arama et al., 2003, 2007; Bader et al., 2010) and microtubule-associated and spindle-relevant proteins, which might be needed for either mitotic or meiotic cell division (Supplementary Table 2).

In agreement with the high transcriptional activity during the 3.5 days of spermatocyte growth and translational activity throughout spermatogenesis, we identified more than 6,000 proteins, many of which are expressed in several tissues. Furthermore, the poly(A) binding protein pAbp and the translational elongation factors Efalpha48D and Ef2B were among the 20 most abundant proteins in larval, pupal and adult testes. Exu, a protein that binds single-stranded RNA, was particularly abundant in pupal testes. In addition, in pupal and adult testis, tubulins were the second most abundant class of proteins, which is consistent with the beginning of the growth of long spermatid flagella in pupal testes. It is important to note that vertebrate testes express high levels of structural proteins, including tubulins, actins and histones (Martyniuk and Alvarez, 2012). Note that the vertebrate testes contain more somatic cell types than *Drosophila* testes, which might explain the high level of histones in vertebrate testes.

### *3.1. Identification of stage-specific proteins confirmed the specificity of the testes proteomes of the different stages*

The spermatocyte stage is the only stage in which Y-chromosomal genes of *Drosophila* are transcribed (for a review, see Piergentili 2010). We identified several proteins encoded by the Y-chromosome. Of these, FDY (Flagrante delicto Y) is enriched in larval testes (Fig. 2C); Carvavalho et al. (2015) showed the testes-specific expression of the corresponding transcript. FDY is predicted to be a hyaluronan/RNA-binding protein, but it is not known whether it is involved in transcriptional or mRNA regulatory processes. Several proteins accumulated from larval to adult stages (Fig. 2C). The Y chromosome is essential for male fertility and encodes male fertility factors. WDY (FBgn0267449), kl-2 (FBgn0001313), kl-3 (FBgn0267432) and kl-5 (Fbgn0267433) were enriched in the proteome of pupal and adult testes (Fig. 2C). We predicted WDY, which contains a WD40 repeat domain, based on expressed sequence tags; and it has been suggested that its encoding gene is *kl-1* (Vibranovski et al., 2008). The male fertility factors encoded by the *kl-2*, *kl-3* and *kl-5* genes encode outer dynein heavy chains of the axoneme (Goldstein et al., 1982; Gepner and Hays, 1993; for a review, see Carvalho et al., 2002). Thus, the abundance of these proteins in pupal and adult testes correlates with the post-meiotic assembly of the axoneme. The Y chromosome transcribes the Mst77Y pseudogenes (Krsticevic et al., 2010; Krsticevic et al., 2015), and the corresponding predicted proteins are very similar to Mst77 F, which is an essential sperm chromatin protein (Jayaramaiah and Renkawitz-

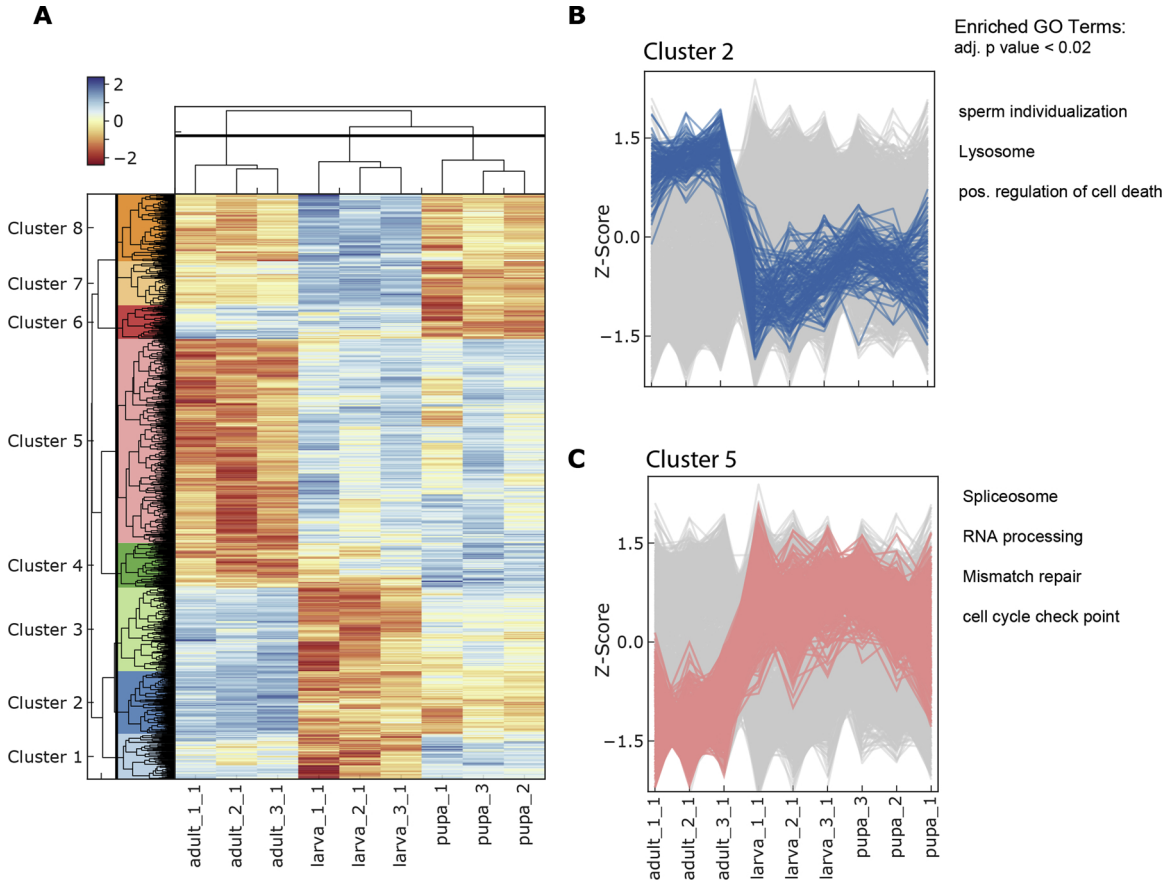


**Fig. 3.** Changes in the proteome during testis development. (A) log2 LFQ intensities of significantly regulated proteins (ANOVA - FDR < 5%) were Z-score transformed and subjected to hierarchical clustering (Euclidean, complete method). Eight clusters were identified (rows) and enriched GO terms were identified using a Fisher Extact test (FDR < 0.05). The complete list of enriched GO terms can be found in the Supplementary Fig. 1. (B–C) Colour coding of members of distinct to clusters 2 and 5 in a line plot. Enriched GO terms are listed next to the plot.

Pohl (2005); Doyen et al., 2015, Kimura and Loppin, 2016). We detected a new protein that corresponds to one of the Mst77Y transcripts, Mst77Y-13 (FBgn0267491).

Mature sperm consist of a head with a length of ca.10 µm; the tail is much longer, ca. 1.8 mm (Fuller, 1993). Thus, we expected that the abundant proteins are mainly part of the flagellum. Accordingly, the outer dense fibre protein of the flagellum Mst98C (FBgn0002865; Appendix) is enriched in adult testes (Schäfer et al., 1993). However, also proteins of the sperm head were enriched in adult proteomes, e.g. Protamine B (FBgn0013301, Supplementary Fig. 1), encoded by *Mst35Bb*. We identified another known sperm chromatin component, Mst77 F (FBgn0086915, Appendix; Jayaramaiah and Renkawitz-Pohl (2005). Also also the acetyl transferase Nejire was identified in all stages, in agreement with its expression in nuclei of spermatocytes and late expression in elongated spermatid nuclei (Hundertmark et al., 2018). Furthermore, the detection of several myosin heavy chain isoforms (Mhc, FBgn0264695, Appendix) in adult testes reflects the presence of the fully developed muscle sheath of the mature organ (Susic-Jung et al., 2012 and references therein).

### 3.2. Cellular and subcellular distribution of newly identified components of nuclei and flagella

Significantly regulated proteins were identified by an analysis of variance using an FDR < 5%, which resulted in approximately 1,850 proteins. Hierarchical clustering of this subset of proteins (Fig. 3A and Supplement Fig. S3) defined eight clusters. To identify overrepresented GO annotation terms in each cluster, we compared cluster specific GO terms to the ones detected in the group of all proteins using a Fisher exact test.. The adult proteome was enriched in components involved in sperm individualization (Fig. 3B; Supplementary Table 3, Noguchi et al., 2006; Fabrizio et al., 1998). By contrast, larval and pupal proteomes were enriched in mRNA splicing components (Fig. 3C), in agreement with the enrichment of transcriptionally active stages before meiotic divisions. These data reflect the enrichment of the developmental stages of male germ cells in the individual testes stages.

### 3.3. CG2046 is present at all stages of testis development and is essential for male fertility

Before concentrating on proteins that are stage-specifically expressed, we analysed in more detail one uncharacterized protein (encoded by *CG2046*) that was detected in all stages. It has been predicted that *CG2046* (FBgn0037378, Fig. 4A, Supplementary Table1) encodes a 25.8 kDa protein; the C-terminal region contains the conserved proteasome assembly chaperone 1 (PSMG1) sequence of mice (Flybase, Gramates et al., 2017; InterPro, Jones et al., 2014). This chaperone in mice binds to the proteasome (for a review, see Murata et al., 2009) and is associated with a proteasome complex (Guruharsha et al., 2011). We named the *CG2046*-encoded protein *Drosophila* Proteasome Assembly Chaperone 1 (dPSMG1). We analysed a $CG2046^{F01807}$ mutant bearing a PiggyBac transposon insertion 85 bp downstream of the translation initiation codon of *dPsmg1* that thus interrupts the open reading frame (Fig. 4B). Homozygous flies were viable. In testes of heterozygous $CG2046^{F01807}$ males, dPSMG1 transcripts were observed from the spermatocyte stage until elongating spermatid stages (Fig. 4C), whereas transcripts were barely detected in homozygous $CG2046^{F01807}$ mutants (Fig. 4D). We conclude that the P-element insertion largely leads to a

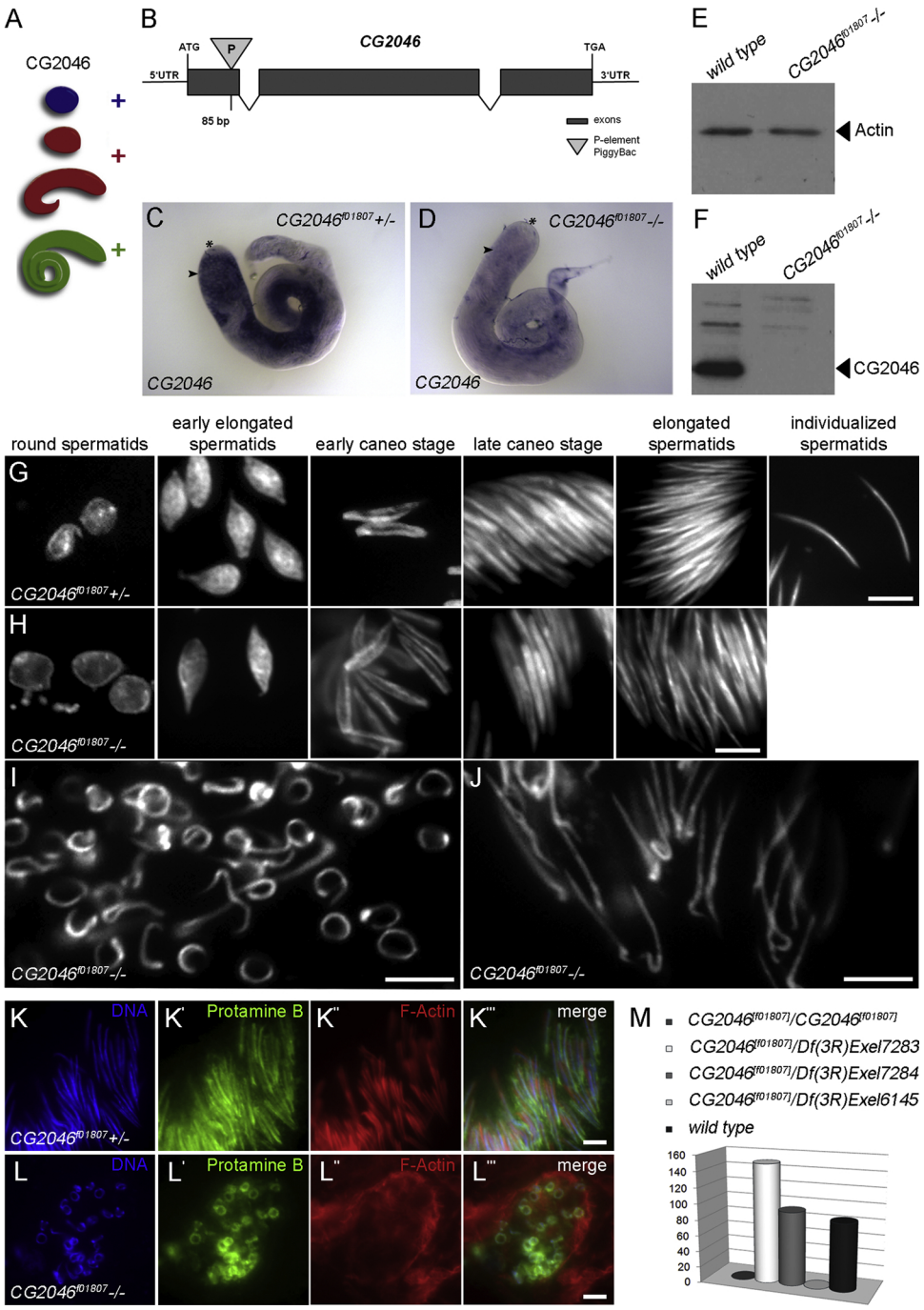


**Fig. 4.** *CG2046* encodes a predicted proteasome assembly chaperone 1 in larval, pupal and adult testes. (A) Presence of the CG2046 protein in the proteome of testes developmental stages. (B) PiggyBac insertion in the coding region of the first exon of *CG2046* in *Drosophila* fly line $CG2046^{f01807}$ (Flybase, Gramates et al., 2017). (C) Detection of *CG2046* transcripts (arrowhead) in the wild-type germ line from spermatogonia to elongated spermatids by *in situ* hybridization with an antisense probe against *CG2046*. (D) Lack of signal (arrowhead) in the male germ line of homozygous $CG2046^{f01807}$ mutants ($CG2046^{f01807}$-/-). (E) Western blot of proteins from testes of wild type and homozygous $CG2046^{f01807}$ -/- males using anti-Actin. (F) Western blot of proteins from testes of ($CG2046^{f01807}$+/-) and homozygous $CG2046^{f01807}$ -/- males using anti-CG2046. (G) Nuclei of post-meiotic germ cell stages from heterozygous $CG2046^{f01807}$ males and (H) homozygous $CG2046^{f01807}$ males visualized by Hoechst staining. (I) Elongated, ring-shaped nuclei of spermatids in some cysts of homozygous $CG2046^{f01807}$ testes. (J) Elongated, bent nuclei of spermatids in some cysts of homozygous $CG2046^{f01807}$ testes. (K–K‴). Nuclei in a cyst of heterozygous $CG2046^{f01807}$ males; (K) DNA visualized by Hoechst staining; (K′) Protamine B staining (green); (K″) Phalloidin staining of individualized actin cones (red); (K‴) merged image of K, K′ and K″. (L–L‴) Misshaped spermatid nuclei of homozygous $CG2046^{01807}$ mutants; (L) DNA visualized by Hoechst staining; (L′) Protamine B staining (green); (L″) phalloidin staining of actin (red); (L‴) merged image of L, L′ and L″. (M) Fertility test of homozygous *CG2046* $^{f01807}$ mutant males, wild-type males and males carrying the *CG2046* mutant allele *in trans* to a deficiency in which *CG2046* is deleted (Df(3R)Exel6145) or not (Df(3R)Exel7283, 7284). The Y axis gives the average number of progeny per male (n = 20 for each genotype). Asterisk marks the hub. Scale bars, 5 µm.

lack of dPSMG1 transcripts. We raised an antibody against a peptide of dPCMG1. This antibody detected a protein of ca. 25 kDa (25.8 kDa predicted, Flybase, Gramates et al., 2017). In agreement with the lack of *CG2046* transcripts, the CG2046 protein was not detected in immunoblots using protein extracts of *CG2046* mutant testes (Fig. 4F; actin loading control shown in Fig. 4E). Notably, our customized anti-dPCMG1 antibody was suitable for immunoblot analysis, but immunofluorescence staining revealed no difference between *CG2046* mutants and controls; thus, the antibody or the fixation procedure is not suitable for standard immunofluorescence.

In testes of *CG2046* mutants, the phenotype manifested very late during spermiogenesis. We found no individualized sperm (compare Fig. 4G and H), and cysts with elongated spermatids shortly before individualization varied in phenotype; some nuclei were similar to those of the wild type (Fig. 4H), some were doughnut shaped (Fig. 4I) and some were bent at one end like a walking stick (Fig. 4J). We asked whether protamines are deposited at the late canoe stage and whether individualization complexes are formed. Protamine B (Fig. 4K′) and the actin-rich individualization cones (visualized by phalloidin staining; Fig. 4K″; merged image in Fig. 4K‴) were clearly present in homozygous $CG2046^{F01807}$ mutants. Protamine B was detected in homozygous $CG2046^{01807}$ mutants (Fig. 4L′), but individualization cones were not detected at the doughnut-shaped nuclei (Fig. 4L″; merged image in Fig. 4L‴). However, we cannot exclude that this aberrant nucleus form is generated after individualization. In accordance with the strong post-meiotic phenotype, homozygous $CG2046^{F01807}$ mutants and $CG2046^{F01807}$ *in trans* to the deletion Exel6145 (where *CG2046* and 15 other genes are deleted) were male sterile (Fig. 4M). *CG2046* $^{F01807}$ *in trans* to other deletions excluding *CG2046* were fertile, which indicated that the sterility is due to disruption of the *CG2046* gene and

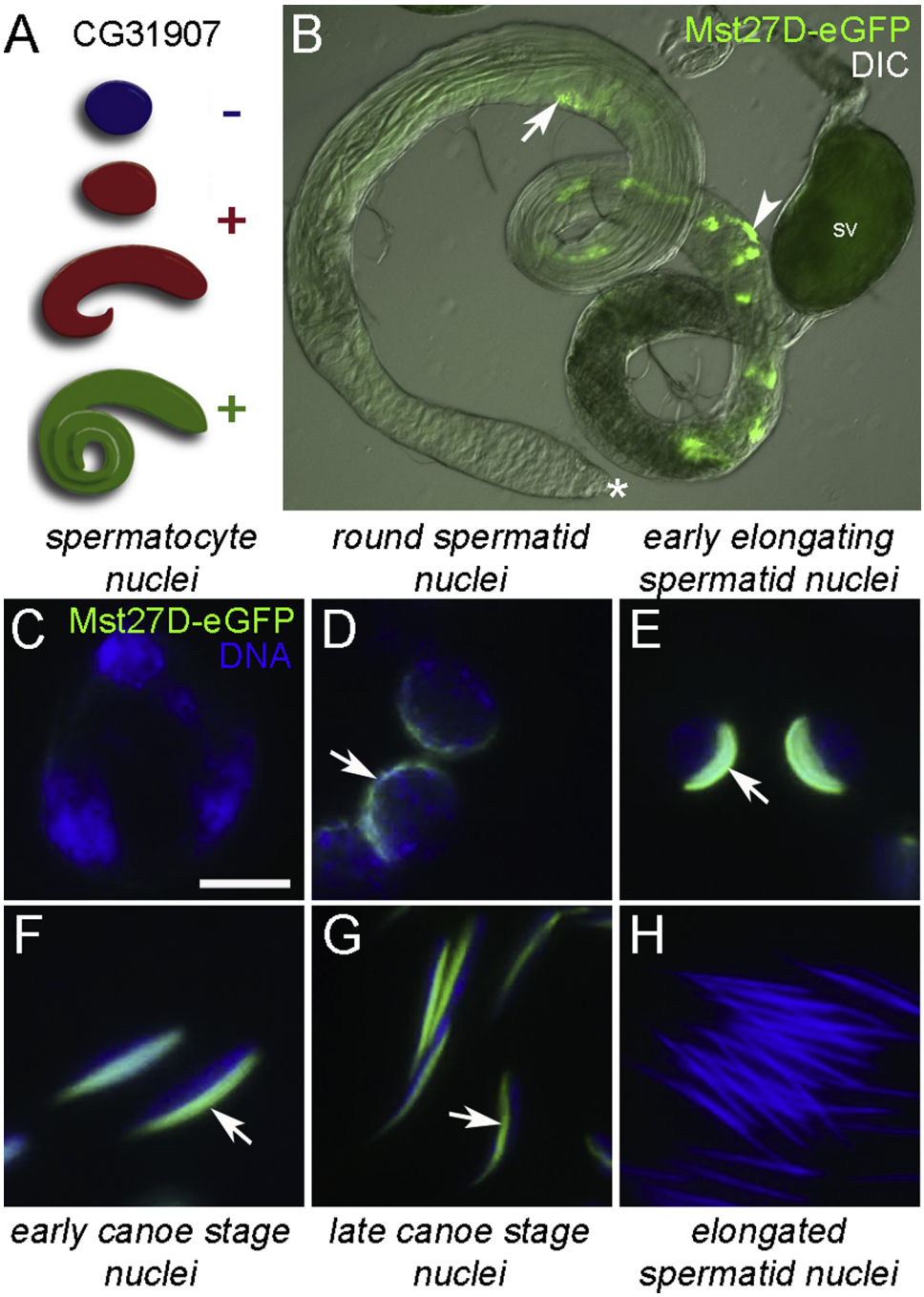


**Fig. 5.** Mst27D-eGFP (CG31907) is detected close to nuclei during nuclear shaping. (A) Presence of CG31907 (Mst27D) in the proteome of testes developmental stages. (B) Detection of Mst27D-eGFP combined with differential interference contrast (DIC) image of adult testes; arrow, shortly after meiosis; arrowhead, close to nuclei of elongated spermatid; asterisk, testis hub; SV, seminal vesicle. (C–H) Analysis of different stages of spermatogenesis in testes squash preparations; (C) spermatocytes; (D) round nuclei; (E) oval nuclei; (F) early canoe stage nuclei; (G) late canoe stage nuclei; (H) nuclei of elongated spermatids. Blue, DNA visualized by Hoechst staining; green, Mst27D-eGFP. Scale bars, 5 µm.

not to second hit events. Thus, we conclude that dPSGM1 is essential for male fertility, and that this is manifested in the nuclear-shaping defects and arrest at the individualization stage.

### 3.4. *Mst27D marks spermatid nuclei during nuclear shaping*

We found CG31907 (FBgn0051907, Appendix) in the testes proteome of pupal and adult males and strongly reduced in that of larval males (Fig. 5A), which indicates a limited protein expression in post-meiotic stages. As the gene is solely transcribed in males and localized at 27D on polytene chromosomes, we named this gene *Male specific transcript 27D (Mst27D)*. It is predicted that *Mst27D* encodes a microtubule-binding protein (Flybase, Gramates et al., 2017). Microtubules are involved in many cellular structures during the development of male germ cells. For example, microtubules are associated with the formation of mitotic and meiotic spindles, centrosomes and axonemes, and are involved in nuclear shaping of the sperm head (Fuller et al., 1988). We constructed a gene encoding an Mst27D-eGFP fusion protein; the established transgenic *Drosophila* strain showed a strong eGFP signal shortly after meiotic divisions (Fig. 5B; arrow). In addition, Mst27D-eGFP was clearly visible along round nuclei of spermatids (Fig. 5B, arrowhead; D, arrow) and prominent during the stages of nuclear elongation (Fig. 5B, arrowhead). We did not observe labelled sperm nuclei in seminal vesicles (Fig. 5B). A closer inspection confirmed that the first clear presence of Mst27D-eGFP was along round spermatid nuclei (Fig. 5D), and it accumulated on one side of the nucleus of early elongating spermatids (Fig. 5E). Early and late canoe stages (Fig. 5F, G) showed Mst27D-eGFP on one side of the elongated nucleus, and Mst27D-eGFP was not detected when nuclei were fully elongated (Fig. 5H). Microtubules play an essential role in nuclear

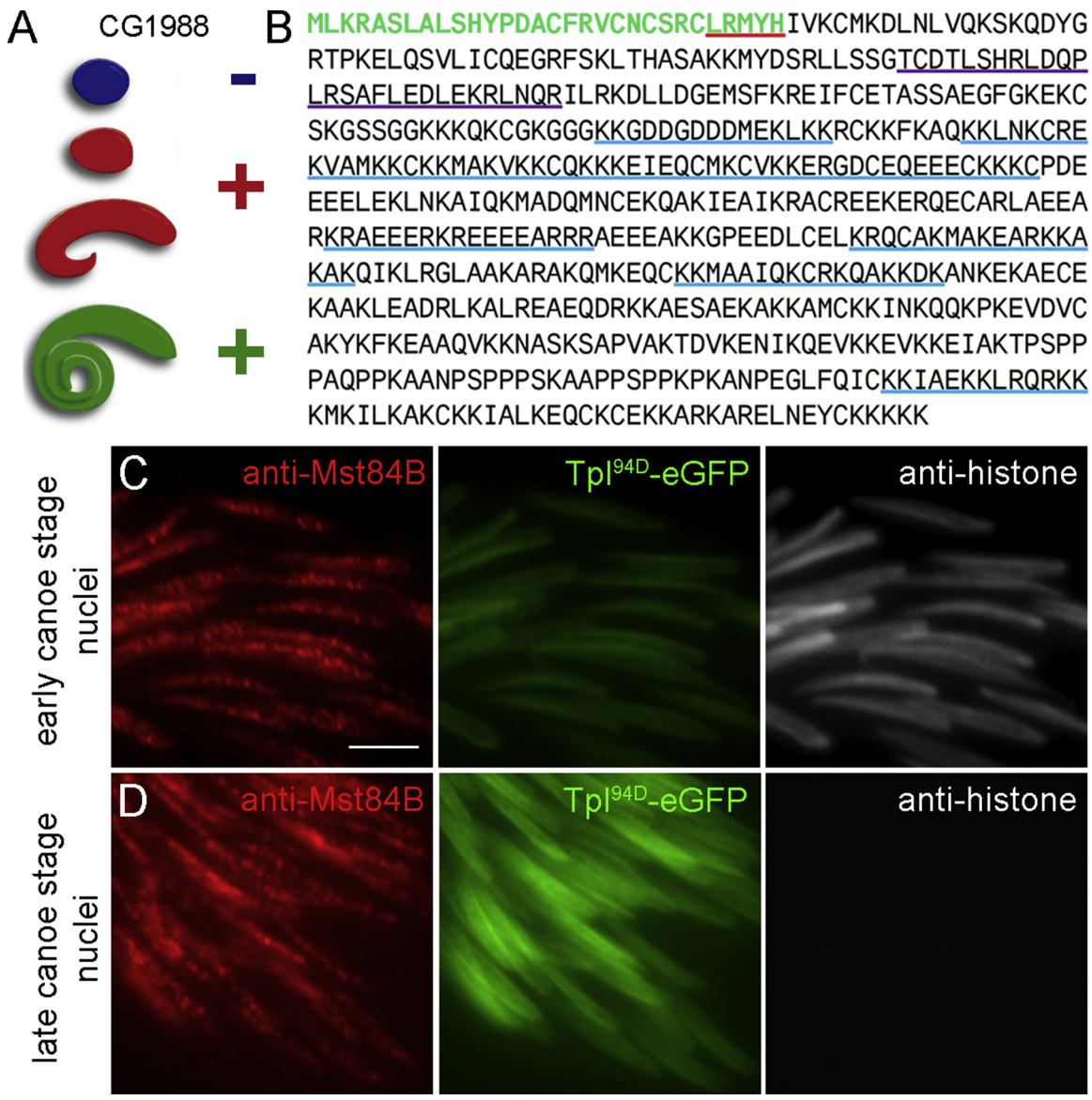


**Fig. 6.** Mst84B (CG1988) is localized during histone-to-protamine transition. (A) Presence of Mst84B in the proteome of testes developmental stages. (B) Amino acid sequence of Mst84B. Green, putative mitochondrial import signal; red underline, mitochondrial peptidase consensus sequence; purple underline, peptide used as antigen for antibody generation; blue, putative nuclear localization signals. (C, D) Localization of Mst84D (red), Tpl94D-eGFP (green), and histones (white) in (C) early and (D) late canoe stages. Scale bar, 5 µm.

shaping (Fuller et al., 1988). Furthermore, β2 tubulin (Tub85D, FBgn0003889, Supplementary Fig. 1) is highly abundant, is a component of the axoneme and is also essential for nuclear shaping (Fuller et al., 1987; Rathke et al., 2010). Sperm-head shaping is also a feature in mammals (for a review, see Wei and Yang, 2018). Mst27D is related to the human microtubule-associated protein MAPRE1, which is a member of the EB1 family proteins (Su and Qi, 2001). It remains to be clarified whether MAPRE1 is characteristic for nuclear shaping in mammals. In summary, we identified a protein, Mst27D, putatively involved in nuclear shaping through interaction with microtubules.

### *3.5. Mst84B contains C-terminal lysine-rich regions and characterizes the spermatid chromatin during the histone-to-protamine transition*

We quantified CG1988 (FBgn0037464) in adult testes but not in larval and pupal testes (Fig. 6A, Supplementary Fig. 1). The protein is rich in cysteine and lysine, which results in a basic pI value of 10.48. Such a high pI is typical for transition proteins and sperm-packaging proteins. It contains multiple putative nuclear localization sites (Fig. 6B), and we considered this protein as a potential candidate for a post-meiotic chromosomal protein. *CG1988* transcripts are limited to males in adult stages; we named this protein *Male specific transcript 84B (Mst84B)* (Flybase, Gramates et al., 2017). Mst84D protein was expressed in a dotted pattern over the spermatid chromatin during the histone-to-protamine transition (Fig. 6C, D). The timing of Mst84B protein expression overlapped with that of histones and the transition-protein-like 94D (Tpl94D) in early canoe stage (Fig. 6C). Both Tpl94D and Mst84B were also detected in the late canoe stage, while histones were not detected (Fig. 6D). At this stage, the exchange of histones starts with transient chromatin components, such as Tpl94D and dimers of tHMG-1 and tHMG-2 (Gärtner et al., 2015) and ends with ProtA (Mst35Ba, FBgn0013300), ProtB (Mst35Bb, FBgn0013301), Mst77 F (FBgn0086915) and Prtl99C (FBgn0039707) (Eren-Ghiani et al., 2015). Hence, the similar expression of Mst84B suggests that Mst84B is also a transient component of chromatin during the transition from a histone-based chromatin to a protamine-based chromatin (for a review on chromatin dynamics during spermiogenesis, see Rathke et al., 2014). This stage is characterized by multiple DNA breaks, (Rathke et al.,

2007) which might facilitate the opening of the chromatin and thus the release of histones, followed by the deposition of transition proteins and protamines (for a review, see Rathke et al., 2014). The expression of Mst84B coincided with DNA breaks, but the signals hardly co-localized (Supplementary Fig. 4B, C). A P-element mutation results in a truncated protein; flies homozygous for this mutation are fertile (Flybase, Gramates et al., 2017). Mutants of Tpl94D were also fertile, as were mutants that lost both tHMG-1 (CG7048) and tHMG-2 (CG7046), which form a transient chromatin component dimer (Gärtner et al., 2015). Thus, we propose that either transition-protein-like proteins are functionally redundant or their loss is compensated by up-regulation of related proteins, as has been suggested to occur at the transcriptional level for HMGZ after loss of tHMG-1 and tHMG-2 (Gärtner et al., 2015).

In summary, the finding that Mst84B is an additional transition-protein-like protein underscores the complexity of chromatin reorganization during the histone-to-protamine transition.

### 3.6. In adult testes, CG5089-eGFP and CG8701-eGFP are detected in elongated flagella

We exemplarily studied other small basic proteins that were solely detected or showed a significant up-regulation in adult flies compared to pupae and larvae (Fig. 7A), as this stage might be enriched in proteins associated with flagella or sperm chromatin. For example, *CG5089* (FBgn0034144) has the coding capacity for a basic protein (Table 1 and Supplementary Fig. 1). We established transgenic *Drosophila* lines that synthesize a CG5089-eGFP fusion protein. Pupal testes at 48 h APF showed no GFP signal in elongated spermatids (Fig. 7B, arrow), in agreement with the results obtained from the pupal proteome. In adult testes, CG5089-eGFP was detected in some but not all bundles of flagella (Fig. 7C, eGFP stained arrow head, unstained spermatids arrow), and the nuclei of elongated spermatids showed no CG5089-eGFP signal (Fig. 7D). Within a cyst, all flagella are unstained or stained.

We detected the cysteine-rich protein CG8701 (FBgn0033287) only in the proteome of adult testes (Fig. 7A, Supplementary Fig. 1), as described in Dorus et al. (2006) and Wasbrough et al. (2010), and the tagged version of CG8701-eGFP protein was restricted to some cysts in adult testes in which all flagella were GFP positive (Fig. 7E-G, arrowhead: eGFP stained, arrow: unstained spermatids).

In conclusion, we identified three flagellar proteins that are synthesized very late during spermiogenesis. These proteins are candidates for outer dense fibre proteins that stabilize the flagella or for regulators of sperm motility.

### 3.7. dTheg is a component of the flagellum and essential for male fertility

Another protein with a restricted and abundant expression in the adult testes is CG6332 (FBgn0038921, Fig. 8A, Supplementary Fig. 1). This protein is related to the Theg (testicular haploid expressed gene) protein of mice, known as THEG in humans. We detected the characteristic repeats of human THEG protein in the *Drosophila* protein (Fig. 8B) and named this protein dTheg.

Earlier, Yanaka et al. (2000) observed abnormally elongated spermatids and spermatids lacking flagella in an insertional Theg mutant mouse model, whereas Mannan et al. (2003) reported a nuclear localization of Theg in spermatids. However, the *Theg* knockout mouse models demonstrated that Theg might be dispensible for mouse spermatogenesis. We established transgenic flies with a gene encoding the fusion protein CG6332-eGFP. The GFP signal was detected in the flagella of very late elongated spermatids and in the flagella of sperm in the seminal vesicles (Supplementary Fig. 5B). We analysed the *CG6332* minos insertion mutant *Mi{ET1}CG6332*$^{MB01798}$ (Flybase, Gramates et al., 2017), for which a C-terminal truncated protein (CG6223-ΔC, 236 aa instead of 353 aa) was predicted (Fig. 8B). We verified the shorter transcript of *Mi{ET1}CG6332*$^{MB01798}$ by RT-PCR. Primers that amplified the 5′ region of the transcripts detected both the full-length and truncated transcript (Fig. 8C), whereas the primers that amplified the 3′ region only detected the full-length transcript (Fig. 8C). A specific antibody raised against a dTheg epitope (anti-CG6332; Fig. 8B) revealed the presence of dTheg in flagella of elongated spermatids (Fig. 8E); DNA co-staining at higher magnification showed that the nuclei are free of dTheg (Fig. 8F). Testes of homozygous *Mi{ET1}CG6332*$^{MB01798}$ mutants contained bundles of elongated spermatids but lacked dTheg (Fig. 8E′), which indicated that the truncated protein is unstable. Moreover, the loss of dTheg caused complete male sterility (n = 20). In agreement with the observed sterility, the seminal vesicles lacked mature sperm (Fig. 8D). Thus, the *Drosophila* dTheg protein is deposited during very late stages in the flagella, which suggests a function during the formation of the mature flagellum. dTheg is required for male fertility.

## 4. Concluding remarks

The stage-specific testes proteomes of *Drosophila* identified

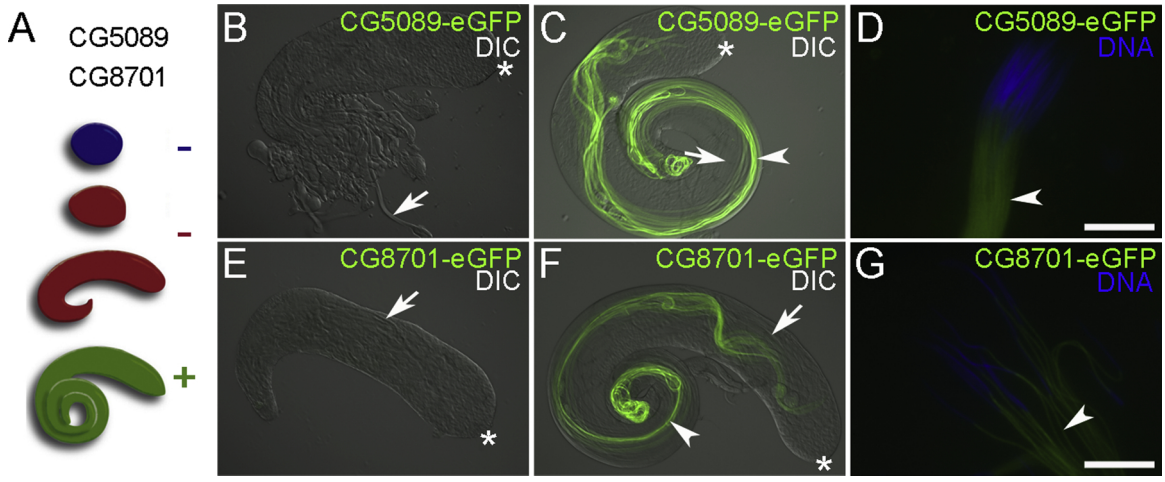


**Fig. 7.** CG5089-eGFP and CG8701-eGFP are synthesized in flagella of late elongating spermatids. (A) Presence of CG5089 and CG8701 in the proteome of testes developmental stages. (B, E) Lack of detection of (B) CG5089-eGFP and (E) CG8071-eGFP in pupal testes 48 h APF in differential interference contrast (DIC) images; arrow, elongating unlabelled flagella. (C, F) Detection of (C) CG5089-eGFP and (F) CG8071-eGFP in adult testes in DIC image; arrowhead, late elongated spermatids; arrow, other unlabelled spermatid bundles. (D, G) Detection of (D) CG5089-eGFP and (G) CG8701-eGFP in adult testes squash preparations; blue, DAPI staining of nuclei; arrowhead, eGFP-labelled flagella. Scale bars, 10 µm.

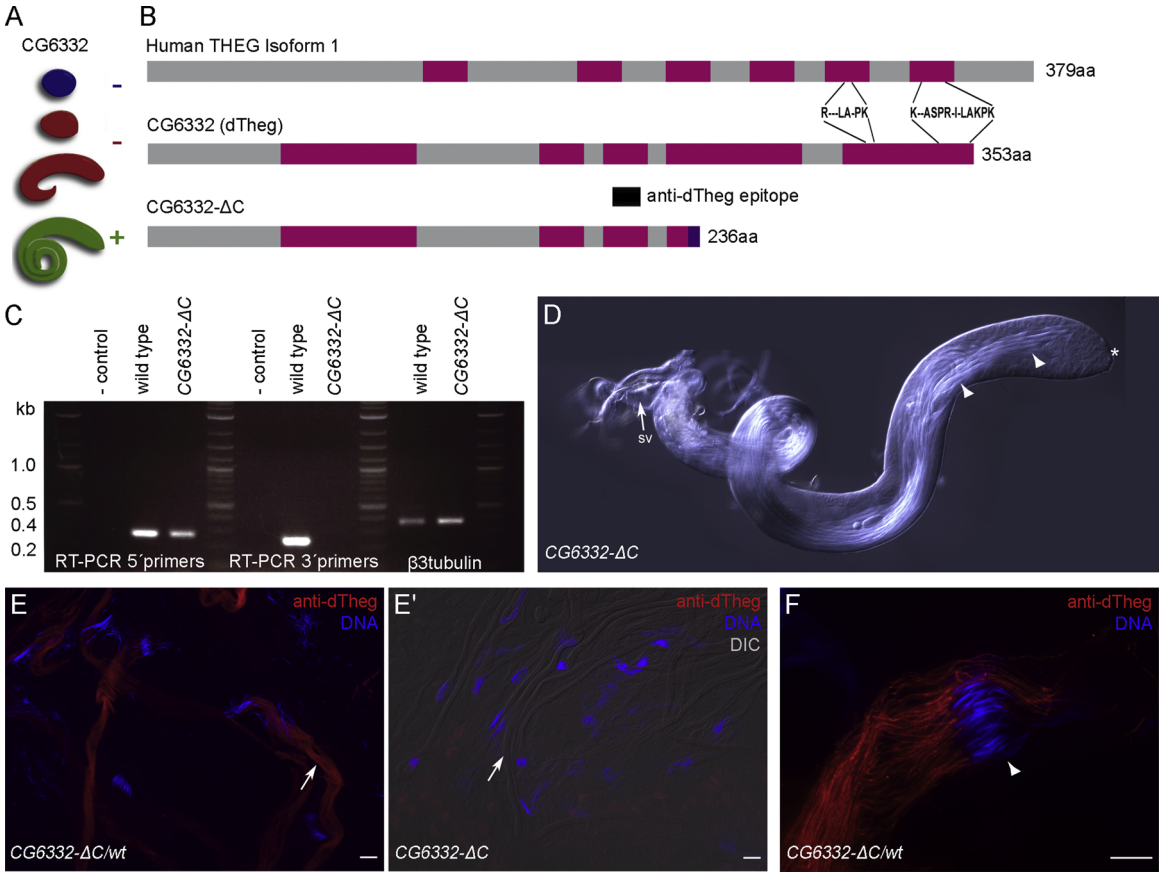


**Fig. 8.** CG6332 (dTheg) is synthesized in flagella in adult testes and resembles the testicular haploid expressed gene protein (THEG) of humans. (A) Presence of CG6332 in the proteome testes developmental stages. (B) Schematic comparison of human THEG protein, the *Drosophila* CG6332 protein (dTheg) and its truncated version CG6332-ΔC. Pink, characteristic human THEG repeat regions; black bar, epitope (CLAKPKKAPKVPKPDRGAGE) used for generating antibody raised against CG6332. (C) RT-PCR analysis of *CG6332* in wild type and *Mi{ET1}CG6332*$^{MB01798}$ (*CG6332-ΔC*) transcripts using RNA isolated from adult testes, and a 5′ primer pair and a 3′ primer pair; transcript of the β3 tubulin gene served as control. (D) Whole-mount of testes isolated from homozygous *Mi{ET1}CG6332*$^{MB01798}$ (*CG6332-ΔC*) males; arrow SV, empty seminal vesicles; arrowheads, elongated flagella; asterisk, testis hub. (E, E′) Differential interference contrast images of (E) heterozygous and (E′) homozygous *Mi{ET1}CG6332*$^{MB01798}$ (*CG6332-ΔC*) males stained with anti-CG6332 (red). Blue, Hoechst staining. (F) Higher magnification of E. Scale bar, 20 µm (E–E′) or 10 µm (F).

**Table 2**
Identified proteins (Table 1) and results of biological experiments concerning these proteins

| Gene | Protein | Stage in which enriched in proteome | Expression | Essential for male fertility |
|---|---|---|---|---|
| *CG12860* | | Adult | n.d. | n.d. |
| *CG4691* | | Pupae<br>Adult | n.d. | n.d. |
| *CG1988* | Mst84B | Adult | During histone-to-protamine transition | no |
| *CG17377* | | Adult | n.d. | n.d. |
| *CG31542* | | Adult | n.d. | n.d. |
| *CG31907* | Mst27D | Pupal, adult | During nuclear shaping | n.d. |

n.d. : not determined.

hundreds of proteins that are enriched before meiotic divisions (larval proteome), in round spermatids and spermatids during elongation of nuclei and flagella (pupal proteome) and in late steps of spermiogenesis, such as protamine deposition and formation of outer dense fibres (adult proteome). Our biological data of some of these proteins confirm the results of proteome analysis (Table 2) and underscore the high potential of testes proteome analysis for future studies of spermatogenesis in *Drosophila*. Our comprehensive quantitative proteome study of *Drosophila* sperm development represents a public repository and will be of great value in the detailed study of sperm development in flies.

## Declarations of conflict of interest

none

## Acknowledgements

We thank Sylvia Jeratsch and Ellen Borowski (Max-Planck-Institut für Herz- und Lungenforschung) for advice and technical assistance on sample preparation for mass spectrometry analysis. We are grateful to Rainer Renkawitz and Katharina Fritzen for critical reading, Karen A. Brune for competent language revision of this manuscript and Katja Gessner for excellent secretarial assistance. We thank Christopher Feldewert for technical help, and Ruth Hyland and Ljubinka Cigoja for

taking care of our fly facility and establishment of transgenic *Drosophila* lines. This work was supported by grants from Deutsche Forschungsgemeinschaft (TRR81 "Chromatin Changes in Differentiation and Malignancies" to R.R.-P. and C.R.) and by REPRO-TRAIN Marie Curie Initial Training Network (Z.E.-G, PITN-2011-289880 to R.R.-P.) and the DFG Excellence Cluster Cardio-Pulmonary System (ECCPS), and the Cologne Cluster of Excellence on Cellular Stress Responses in Aging-associated Diseases (CECAD to M. K).

## Appendix A. Supplementary data

Supplementary material related to this article can be found, in the online version, at doi:https://doi.org/10.1016/j.ejcb.2019.01.001.

## References

Arama, E., Agapite, J., Steller, H., 2003. Caspase activity and a specific cytochrome C are required for sperm differentiation in Drosophila. Dev Cell 4, 687–697.
Arama, E., Bader, M., Rieckhof, G.E., Steller, H., 2007. A ubiquitin ligase complex regulates caspase activation during sperm differentiation in Drosophila. PLoS Biol 5, e251.
Amaral, A., Castillo, J., Ramalho-Santos, J., Oliva, R., 2014. The combined human sperm proteome: cellular pathways and implications for basic and clinical science. Hum Reprod Update 20, 40–62.
Awe, S., Renkawitz-Pohl, R., 2010. Histone H4 acetylation is essential to proceed from a histone- to a protamine-based chromatin structure in spermatid nuclei of Drosophila melanogaster. Syst Biol Reprod Med 56, 44–61.
Bader, M., Arama, E., Steller, H., 2010. A novel F-box protein is required for caspase activation during cellular remodeling in Drosophila. Development 137, 1679–1688.
Barckmann, B., Chen, X., Kaiser, S., Jayaramaiah-Raja, S., Rathke, C., Dottermusch-Heidel, C., Fuller, M.T., Renkawitz-Pohl, R., 2013. Three levels of regulation lead to protamine and Mst77F expression in Drosophila. Dev Biol 377, 33–45.
Carvavalho, A.B., Vicosa, B., Russo, C.A., Swenor, B., Clark, A.G., 2015. Birth of a new gene on the Y chromosome of Drosophila melanogaster. Proc Natl Acad Sci USA 112, 12450–12455.
Cox, J., Mann, M., 2008. MaxQuant enables high peptide identification rates, individualized p.p.b.-range mass accuracies and proteome-wide protein quantification. Nat Biotechnol 26, 1367–1372.
Cox, J., Neuhauser, N., Michalski, A., Scheltema, R.A., Olsen, J.V., Mann, M., 2011. Andromeda: a peptide search engine integrated into the MaxQuant environment. J Proteome Res 10, 1794–1805.
Doggett, K., Jiang, J., Aleti, G., White-Cooper, H., 2011. Wake-up-call, a lin-52 paralogue, and Always early, alin-9 homologue physically interact, but have opposite functions in regulating testis-specific gene expression. Dev. Bio.l 355, 381–393.
Dorus, S., Busby, S.A., Gerike, U., Shabanowitz, J., Hunt, D.F., Karr, T.L., 2006. Genomic and functional evolution of the *Drosophila melanogaster* sperm proteome. Nat Genet 38, 1440–1445.
Doyen, C.M., Chalkley, G.E., Voets, O., Bezstarosti, K., Demmers, J.A., Moshkin, Y.M., Verrijzer, C.P., 2015. A testis-specific chaperone and the chromatin remodeler ISWI mediate repackaging of the paternal genome. Cell Rep 13, 1310–1318.
Doyen, C.M., Moshkin, Y.M., Chalkley, G.E., Bezstarosti, K., Demmers, J.A., Rathke, C., Renkawitz-Pohl, R., Verrijzer, C.P., 2013. Subunits of the histone chaperone CAF1 also mediate assembly of protamine-based chromatin. Cell Rep 4, 59–65.
Eren-Ghiani, Z., Rathke, C., Theofel, I., Renkawitz-Pohl, R., 2015. Prtl99C acts together with protamines and safeguards male fertility in Drosophila. Cell Rep 13, 2327–2335.
Fabrizio, J.J., Hime, G., Lemmon, S.K., Bazinet, C., 1998. Genetic dissection of sperm individualization in Drosophila melanogaster. Development 125, 1833–1843.
Fuller, M.T., 1993. Spermatogenesis. In: Bate, M., Martinez-Arias, A. (Eds.), The development of *Drosophila melanogaster*. Cold Spring Harbor Laboratory Press, Cold Spring Harbor, New York, pp. 71–147.
Fuller, M.T., Caulton, J.H., Hutchens, J.A., Kaufman, T.C., Raff, E.C., 1987. Genetic analysis of microtubule structure: a beta-tubulin mutation causes the formation of aberrant microtubules in vivo and in vitro. J Cell Biol 104, 385–394.
Fuller, M.T., Caulton, J.H., Hutchens, J.A., Kaufman, T.C., Raff, E.C., 1988. Mutations that encode partially functional beta 2 tubulin subunits have different effects on structurally different microtubule arrays. J Cell Biol 107, 141–152.
Gärtner, S.M., Rathke, C., Renkawitz-Pohl, R., Awe, S., 2014. Ex vivo culture of *Drosophila* pupal testis and single male germ-line cysts: dissection, imaging, and pharmacological treatment. J Vis Exp 51868.
Gärtner, S.M., Rothenbusch, S., Buxa, M.K., Theofel, I., Renkawitz, R., Rathke, C., Renkawitz-Pohl, R., 2015. The HMG-box-containing proteins tHMG-1 and tHMG-2 interact during the histone-to-protamine transition in Drosophila spermatogenesis. Eur J Cell Biol 94, 46–59.
Gepner, J., Hays, T.S., 1993. A fertility region on the Y chromosome of *Drosophila melanogaster* encodes a dynein microtubule motor. Proc Natl Acad Sci U S A 90, 11132–11136.
Goldstein, L.S., Hardy, R.W., Lindsley, D.L., 1982. Structural genes on the Y chromosome of Drosophila melanogaster. Proc Natl Acad Sci U S A 79, 7405–7409.
Grmai, L., Hudry, B., Miguel-Aliaga, I., Bach, E.A., 2018. Chinmo revents transformer alternative splicing to maintain sex identity. OLoS Genti. 14, e1007203.
Gramates, L.S., Marygold, S.J., Santos, G.D., Urbano, J.M., Antonazzo, G., Matthews, B.B., Rey, A.J., Tabone, C.J., Crosby, M.A., Emmert, D.B., Falls, K., Goodman, J.L., Hu, Y., Ponting, L., Schroeder, A.J., Strelets, V.B., Thurmond, J., Zhou, P., the FlyBase, C, 2017. FlyBase at 25: looking to the future. Nucleic Acids Res 45, D663–D671.
Guruharsha, K.G., Rual, J.F., Zhai, B., Mintseris, J., Vaidya, P., Vaidya, N., Beekman, C., Wong, C., Rhee, D.Y., Cenaj, O., McKillip, E., Shah, S., Stapleton, M., Wan, K.H., Yu, C., Parsa, B., Carlson, J.W., Chen, X., Kapadia, B., VijayRaghavan, K., Gygi, S.P., Celniker, S.E., Obar, R.A., Artavanis-Tsakonas, S., 2011. A protein complex network of Drosophila melanogaster. Cell 147, 690–703.
Hoffmann, A.A., Turelli, M., 1988. Unidirectional incompatibility in *Drosophila simulans*: inheritance, geographic variation and fitness effects. Genetics 119, 435–444.
Huang, S.Y., Lin, J.H., Chen, Y.H., Chuang, C.K., Lin, E.C., Huang, M.C., Sunny Sun, H.F., Lee, W.C., 2005. A reference map and identification of porcine testis proteins using 2-DE and MS. Proteomics 5, 4205–4212.
Huang, S.Y., Lin, J.H., Teng, S.H., Sun, H.S., Chen, Y.H., Chen, H.H., Liao, J.Y., Chung, M.T., Chen, M.Y., Chuang, C.K., Lin, E.C., Huang, M.C., 2011. Differential expression of porcine testis proteins during postnatal development. Anim Reprod Sci 123, 221–233.
Hundertmark, T., Gärtner, S.M.K., Rathke, C., Renkawitz-Pohl, R., 2018. Nejire/dCBP-mediated histone H3 acetylation during spermatogenesis is essential for male fertility in Drosophila melanogaster. PLoS One 13, e0203622.
Hundertmark, T., Kreutz, S., Merle, N., Nist, A., Lamp, B., Stiewe, T., Brehm, A., Renkawitz-Pohl, R., Rathke, C., 2019. Drosophila melanogaster tPlus3a and tPlus3b ensure full male fertility by regulating transcription of Y-chromosomal sperm fluidity, and heat shock genes. unpublished results. .
Huttlin, E.L., Jedrychowski, M.P., Elias, J.E., Goswami, T., Rad, R., Beausoleil, S.A., Villen, J., Haas, W., Sowa, M.E., Gygi, S.P., 2010. A tissue-specific atlas of mouse protein phosphorylation and expression. Cell 143, 1174–1189.
Jayaramaiah, S., Renkawitz-Pohl, R., 2005. Replacement by *Drosophila melanogaster* protamines and Mst77F of histones during chromatin condensation in late spermatids and role of sesame in the removal of these proteins from the male pronucleus. Mol Cell Biol 25, 6165–6177.
Jones, P., Binns, D., Chang, H.Y., Fraser, M., Li, W., McAnulla, C., McWilliam, H., Maslen, J., Mitchell, A., Nuka, G., Pesseat, S., Quinn, A.F., Sangrador-Vegas, A., Scheremetjew, M., Yong, S.Y., Lopez, R., Hunter, S., 2014. InterProScan 5: genome-scale protein function classification. Bioinformatics 30, 1236–1240.
Karr, T.L., 2007. Fruit flies and the sperm proteome. Hum Mol Genet 16 Spec 2, R124–133.
Kimura, S., Loppin, B., 2016. The *Drosophila* chromosomal protein Mst77F is processed to generate an essential component of mature sperm chromatin. Open Biol 6.
Krsticevic, F.J., Santos, H.L., Januario, S., Schrago, C.G., Carvalho, A.B., 2010. Functional copies of the Mst77F gene on the Y chromosome of Drosophila melanogaster. Genetics 184, 295–307.
Krsticevic, F.J., Schrago, C.G., Carvalho, A.B., 2015. Long-Read single molecule sequencing to resolve tandem gene copies: The Mst77Y region on the *Drosophila melanogaster* Y Chromosome. G3 (Bethesda) 5, 1145–1150.
Leser, K., Awe, S., Barckmann, B., Renkawitz-Pohl, R., Rathke, C., 2012. The bromodomain-containing protein tBRD-1 is specifically expressed in spermatocytes and is essential for male fertility. Biol Open 1, 597–606.
Li, J., Liu, F., Liu, X., Liu, J., Zhu, P., Wan, F., Jin, S., Wang, W., Li, N., Liu, J., Wang, H., 2011. Mapping of the human testicular proteome and its relationship with that of the epididymis and spermatozoa. Mol Cell Proteomics 10 M110 004630.
Liu, M., Hu, Z., Qi, L., Wang, J., Zhou, T., Guo, Y., Zeng, Y., Zheng, B., Wu, Y., Zhang, P., Chen, X., Tu, W., Zhang, T., Zhou, Q., Jiang, M., Guo, X., Zhou, Z., Sha, J., 2013. Scanning of novel cancer/testis proteins by human testis proteomic analysis. Proteomics 13, 1200–1210.
Liu, Y., Ge, Q., Chan, B., Liu, H., Singh, S.R., Manley, J., Lee, J., Weidemann, A.M., Hou, G., Hou, S.X., 2016. Whole animal genome-wide RNAi screen identifies networks regulating germline stem cells in Drosophila. Nat. Commun 7, 121149.
Lu, C., Fuller, M.T., 2015. Recruitment of mediator complex by cell type and stage-specific factors required for tissue-specific TAF dependent gene activation in an adult stem cell lineage. PLoS Genet 11, e1005701.
Ma, Q., de Cuevas, M., Matunis, E.L., 2016. Chinmo is sufficient to induce male fate in somatic cells of the adult *Drosophila* ovary. Development 143, 754–763.
Mannan, A.U., Nayernia, K., Mueller, C., Burfeind, P., Adham, I.M., Engel, W., 2003. Male mice lacking the Theg (testicular haploid expressed gene) protein undergo normal spermatogenesis and are fertile. Biol Reprod 69, 788–796.
Morris, C.A., Benson, E., White-Cooper, H., 2009. Determination of gene expression patterns using in situ hybridization to *Drosophila* testes. Nat Protoc 4, 1807–1819.
Murata, S., Yashiroda, H., Tanaka, K., 2009. Molecular mechanisms of proteasome assembly. Nat Rev Mol Cell Biol 10, 104–115.
Noguchi, T., Lenartowska, M., Miller, K.G., 2006. Myosin VI stabilizes an actin network during *Drosophila* spermatid individualization. Mol Biol Cell 17, 2559–2571.
Nogueira, C., Kashevsky, H., Pinto, B., Clarke, A., Orr-Weaver, T.-L., 2014. Regulation of centromere localization of the *Drosophila* Shugoshin MEI-S332 and sister-chromatid cohesion in meiosis. G3 (Bethesda) 4, 1849–1858.
Nolte, H., MacVicar, T.D., Tellkamp, F., Kruger, M., 2018. Instant Clue: A software suite for interactive data visualization and analysis. Sci Rep 8, 12648.
Paz, M., Morin, M., Del Mazo, J., 2006. Proteome profile changes during mouse testis development. Comp Biochem Physiol Part D Genomics Proteomics 1, 404–415.
Piergentili, R., 2010. Multiple roles of the Y chromosome in the biology of Drosophila melanogaster. ScientificWorldJournal 10, 1749–1767.
Rappsilber, J., Ishihama, Y., Mann, M., 2003. Stop and go extraction tips for matrix-assisted laser desorption/ionization, nanoelectrospray, and LC/MS sample pretreatment in proteomics. Anal Chem 75, 663–670.
Rathke, C., Baarends, W.M., Awe, S., Renkawitz-Pohl, R., 2014. Chromatin dynamics during spermiogenesis. Biochim Biophys Acta 1839, 155–168.

Rathke, C., Baarends, W.M., Jayaramaiah Raja, S., Bartkuhn, M., Renkawitz, R., Renkawitz-Pohl, R., 2007. Transition from a nucleosome-based to a protamine-based chromatin configuration during spermiogenesis in Drosophila. J Cell Sci 120, 1689–1700.

Rathke, C., Barckmann, B., Burkhard, S., Jayaramaiah Raja, S., Roote, J., Renkawitz-Pohl, R., 2010. Distinct functions of Mst77F and protamines in nuclear shaping and chromatin condensation during *Drosophila* spermiogenesis. Eur J Cell Biol 89, 326–338.

Renkawitz-Pohl, R., Hollmann, M., Hempel, L., Schäfer, M.A., 2005. Spermatogenesis. In: Gilbert, L.I., Iatrou, K., Gill, S.S. (Eds.), Comprehensive Molecular Insect Science. Elsevier BV, pp. 157–177.

Rothenbusch-Fender, S., Fritzen, K., Bischoff, M.C., Buttgereit, D., Oenel, S.F., Renkawitz-Pohl, R., 2017. Myotube migration to cover and shape the testis of *Drosophila* depends on Heartless. Cadherin/Catenin, and myosin II. Biol Open 6, 1876–1888.

Schäfer, M., Börsch, D., Hülster, A., Schäfer, U., 1993. Expression of a gene duplication encoding conserved sperm tail proteins is translationally regulated in Drosophila melanogaster. Mol Cell Biol 13, 1708–1718.

Schultz, N., Hamra, F.K., Garbers, D.L., 2003. A multitude of genes expressed solely in meiotic or postmeiotic spermatogenic cells offers a myriad of contraceptive targets. Proc Natl Acad Sci U S A 100, 12201–12206.

Su, L.K., Qi, Y., 2001. Characterization of human MAPRE genes and their proteins. Genomics 71, 142–149.

Susic-Jung, L., Hornbruch-Freitag, C., Kuckwa, J., Rexer, K.H., Lammel, U., Renkawitz-Pohl, R., 2012. Multinucleated smooth muscles and mononucleated as well as multinucleated striated muscles develop during establishment of the male reproductive organs of Drosophila melanogaster. Dev Biol 370, 86–97.

Takemori, N., Yamamoto, M.T., 2009. Proteome mapping of the *Drosophila melanogaster* male reproductive system. Proteomics 9, 2484–2493.

Theofel, I., Bartkuhn, M., Boettger, T., Gartner, S.M.K., Kreher, J., Brehm, A., Rathke, C., 2017. tBRD-1 and tBRD-2 regulate expression of genes necessary for spermatid differentiation. Biol Open 6, 439–448.

Theofel, I., Bartkuhn, M., Hundertmark, T., Boettger, T., Gartner, S.M., Leser, K., Awe, S., Schipper, M., Renkawitz-Pohl, R., Rathke, C., 2014. tBRD-1 selectively controls gene activity in the *Drosophila* testis and interacts with two new members of the bromodomain and extra-terminal (BET) family. PLoS One 9, e108267.

Tyanova, S., Temu, T., Cox, J., 2016a. The MaxQuant computational platform for mass spectrometry-based shotgun proteomics. Nat Protoc 11, 2301–2319.

Tyanova, S., Temu, T., Sinitcyn, P., Carlson, A., Hein, M.Y., Geiger, T., Mann, M., Cox, J., 2016b. The Perseus computational platform for comprehensive analysis of (prote) omics data. Nat Methods 13, 731–740.

Vibranovski, M.D., Koerich, L.B., Carvalho, A.B., 2008. Two new Y-linked genes in Drosophila melanogaster. Genetics 179, 2325–2327.

Vibranovski, M.D., Lopes, H.F., Karr, T.L., Long, M., 2009. Stage-specific expression profiling of *Drosophila* spermatogenesis suggests that meiotic sex chromosome inactivation drives genomic relocation of testis-expressed genes. PLoS Genet 5, e1000731.

Vizcaino, J.A., Csordas, A., del-Toro, N., Dianes, J.A., Griss, J., Lavidas, I., Mayer, G., Perez-Riverol, Y., Reisinger, F., Ternent, T., Xu, Q.W., Wang, R., Hermjakob, H., 2016. 2016 update of the PRIDE database and its related tools. Nucleic Acids Res 44, D447–456.

Wakimoto, B.T., Lindsley, D.L., Herrera, C., 2004. Toward a comprehensive genetic analysis of male fertility in Drosophila melanogaster. Genetics 167, 207–216.

Wasbrough, E.R., Dorus, S., Hester, S., Howard-Murkin, J., Lilley, K., Wilkin, E., Polpitiya, A., Petritis, K., Karr, T.L., 2010. The *Drosophila melanogaster* sperm proteome-II (DmSP-II). J Proteomics 73, 2171–2185.

Wei, Y.L., Yang, W.X., 2018. The acroframosome-acroplaxome-manchette axis may function in sperm head shaping and male fertility. Gene 660, 28–40.

White-Cooper, H., Davidson, I., 2011. Unique aspects of transcription regulation in male germ cells. Cold Spring Harb Perspect Biol 3.

Xiao, P., Tang, A., Yu, Z., Gui, Y., Cai, Z., 2008. Gene expression profile of 2058 spermatogenesis-related genes in mice. Biol Pharm Bull 31, 201–206.

Yanaka, N., Kobayashi, K., Wakimoto, K., Yamada, E., Imahie, H., Imai, Y., Mori, C., 2000. Insertional mutation of the murine kisimo locus caused a defect in spermatogenesis. J Biol Chem 275, 14791–14794.

Zheng, Y., Wang, J.L., Liu, C., Wang, C.P., Walker, T., Wang, Y.F., 2011. Differentially expressed profiles in the larval testes of Wolbachia infected and uninfected Drosophila. BMC Genomics 12, 595.

Zhu, Y.F., Cui, Y.G., Guo, X.J., Wang, L., Bi, Y., Hu, Y.Q., Zhao, X., Liu, Q., Huo, R., Lin, M., Zhou, Z.M., Sha, J.H., 2006. Proteomic analysis of effect of hyperthermia on spermatogenesis in adult male mice. J Proteome Res 5, 2217–2225.